The protease interpain A of *Prevotella intermedia* promotes human oral squamous cell carcinoma cells proliferation and migration

Szu-Min Chang[1*], I-Hsiu Huang[2*], Yun-Jhen Ciou[3], Wen-Rong Wang[3], Ni-Hung Wu[3], Chih-Pin Chuu[4], Jenn-Ren Hsiao[5], Jeffrey S Chang[6], Jang-Yang Chang [7,8], Jenn-Wei Chen[1, 3, 9]

[1] Institute of Basic Medical Sciences, College of Medicine, National Cheng Kung University, Tainan 70101, Taiwan
[2] Department of Biochemistry and Microbiology, Oklahoma State University Center for Health Sciences, Tulsa, OK 74107, USA.
[3] Department of Microbiology and Immunology, College of Medicine, National Cheng Kung University, Tainan 70101, Taiwan
[4] Institute of Cellular and System Medicine, National Health Research Institutes, Miaoli 35053, Taiwan
[5] Department of Otolaryngology, National Cheng Kung University Hospital, Tainan 70101, Taiwan
[6] National Institute of Cancer Research, National Health Research Institutes, Tainan 70101, Taiwan
[7] Institute of Biotechnology and Pharmaceutical Research, National Health Research Institutes, Miaoli 35053, Taiwan
[8] TMU Research Center of Cancer Translational Medicine, Taipei Medical University, Taipei 110301, Taiwan
[9] Center of Infectious Disease and Signaling Research, National Cheng Kung University, Tainan 70101, Taiwan

[*] These authors contributed equally to this article.

Running title: Interpain A promotes OSCC cells proliferation and migration

Key words: *Prevotella intermedia*; OSCC, interpain A; PAR-2

Corresponding Author: Jenn-Wei Chen, Department of Microbiology and Immunology, College of Medicine, National Cheng Kung University, Tainan 70101, Taiwan. E-mail: jc923@mail.ncku.edu.tw

Competing Interest Statement: The authors declare no potential conflicts of interest.

Abstract

Prevotella intermedia has been increasingly recognized as a potential contributor to oral squamous cell carcinoma (OSCC), yet the underlying mechanisms remain poorly defined. In this study, we identified interpain A (InpA), a cysteine protease secreted by *P. intermedia*, as a key virulence factor that promotes oral epithelial cell proliferation and OSCC cell migration. Conditioned medium (CM) derived from *P. intermedia* strain ATCC 25611 enhanced proliferation in both normal oral keratinocytes (SG cells) and OSCC cell lines (SCC-15, SAS). The pro-proliferative effect was abolished upon heat inactivation of the CM and inhibited by E64, a cysteine protease inhibitor, and FSLLRY-NH_2, a PAR-2 antagonist, suggesting the involvement of protease-activated receptor-2 (PAR-2) signaling. InpA was highly secreted by strain ATCC 25611 but not by clinical isolates lacking proliferative effects, and RT-qPCR confirmed higher *inpA* expression in OSCC-derived strains compared to non-cancer controls. Recombinant InpA (rInpA) mimicked the effect of CM, inducing proliferation and migration, which were blocked by PAR-2 inhibition. Transcriptomic and protein-level screening in SG cells revealed activation of EGFR and downstream RAS–RAF–MEK–ERK signaling. Furthermore, in a colorectal cancer (CRC) mouse model, oral administration of *P. intermedia* led to increased tumor formation, suggesting a broader oncogenic potential. These findings highlight InpA as a PAR-2–activating protease that may contribute to OSCC and potentially other cancers associated with oral microbiota dysbiosis.

64 ## Introduction

65 Oral squamous cell carcinoma (OSCC) is a common malignancy worldwide and
66 ranks as the fourth most prevalent cancer among men in Taiwan (1). It represents the
67 most frequent form of head and neck cancer and can develop in various parts of the
68 oral cavity, including the lips, tongue, cheeks, palate, and throat. The majority of oral
69 cancers are squamous cell carcinomas, which are associated with poor prognosis and
70 high mortality, with a 5-year survival rate of approximately 50%. Numerous factors
71 contribute to OSCC development, such as gender, human papillomavirus (HPV)
72 infection, alcohol consumption, tobacco use, betel nut chewing, poor oral hygiene, and
73 alterations in the oral microbiota (2, 3). Notably, chronic periodontitis, a gum disease
74 characterized by gingival inflammation and tooth loss, has been strongly linked to oral
75 cancer (4). Poor oral hygiene facilitates the formation of biofilms, known as dental
76 plaques, which contribute to oral microbiota dysbiosis. Anaerobic bacteria residing
77 within these plaques produce acids and other virulence factors that contribute to
78 periodontal inflammation and disease (5). Anaerobic bacteria residing within these
79 plaques produce acids and other virulence factors that contribute to periodontal
80 inflammation and disease.

81 Several bacterial genera, including *Porphyromonas*, *Fusobacterium*, and
82 *Prevotella*, are found in higher abundance in patients with periodontitis compared to
83 healthy individuals. (6, 7). *Porphyromonas gingivalis*, a Gram-negative anaerobe, is
84 associated with periodontal disease and systemic conditions such as Alzheimer's
85 disease (8). Studies have also linked *P. gingivalis* to various cancers, including lung,
86 pancreatic, prostate, colorectal cancer (CRC), and OSCC (9, 10). This bacterium
87 produces multiple virulence factors, such as lipopolysaccharides (LPS), outer
88 membrane vesicles (OMVs), capsules, and gingipains—cysteine proteases implicated

89 in promoting tumor invasion and migration (11). Another oral bacterium,
90 *Fusobacterium nucleatum*, another Gram-negative anaerobic bacterium, has been
91 associated with CRC, breast, pancreatic, and oral cancers (12, 13). It secretes virulence
92 factors including OMVs, LPS, and adhesins. The adhesin FadA interacts with E-
93 cadherin to activate WNT/β-catenin signaling and promote cell proliferation (14).
94 While Fap2 binds tumor-associated oligosaccharides and the immune checkpoint
95 receptor TIGIT, potentially facilitating immune evasion (15). While much attention has
96 focused on *P. gingivalis* and *F. nucleatum* in OSCC, the role of *Prevotella intermedia*
97 remains poorly understood. *P. intermedia* is a Gram-negative, obligate anaerobic rod-
98 shaped bacterium that requires vitamin K and hemin for growth and is associated with
99 periodontal disease and acute necrotizing ulcerative gingivitis. Recent studies have
100 reported elevated levels of *P. intermedia* in the oral microbiota of OSCC patients
101 compared to healthy controls. Although this correlation suggests a potential role in oral
102 carcinogenesis, the molecular contributions of this association remain unclear.
103 In this study, we demonstrate that *P. intermedia* strain ATCC 25611 promotes
104 proliferation of normal oral epithelial cells (SG cell line) at a multiplicity of infection
105 (MOI) of 100. Its conditioned medium (CM) also enhanced proliferation in SG, SCC-
106 15, and SAS cell lines. Proteomic analysis using capillary electrophoresis/liquid
107 chromatography-mass spectrometry (CE/LC-MS) revealed that a cysteine protease,
108 interpain A (InpA), secreted by strain ATCC 25611, may be the critical factor driving
109 this effect. In addition to stimulating proliferation, InpA also enhanced migration of
110 OSCC cells. Furthermore, in a murine colorectal cancer model, colonization with *P.*
111 *intermedia* increased tumor burden. These findings support a role for *P. intermedia*,
112 and specifically InpA, in promoting OSCC development.
113

114 ## Materials and methods

115 **Bacterial strains and cultures**

116 *P. intermedia* strain ATCC 25611 was obtained from the Bioresource Collection and
117 Research Center (BCRC, Taiwan), and culture conditions were adapted from a
118 previously published protocol (16). Bacteria were grown anaerobically at 37 °C in
119 supplemented Tryptic Soy Broth (ATCC 2722), consisting of tryptic soy broth
120 (#211825, BD) enriched with 0.5% yeast extract (#212750, BD), 0.05% L-cysteine
121 (#A3694, Applichem Panreac), 0.1% hemin (#H9039, Sigma), and 0.02% menadione
122 (#M5625, Sigma). Clinical isolates of *P. intermedia* were obtained from the saliva of
123 patients at National Cheng Kung University Hospital (NCKUH), under Institutional
124 Review Board approval (IRB no. B-ER-106-234). Saliva samples were diluted in PBS
125 and plated on Kanamycin-Vancomycin Laked Blood (KVLB) agar (TPM, Yilan,
126 Taiwan). After 2–3 days of anaerobic incubation (5% CO_2, 5% H_2, 90% N_2), black-
127 pigmented colonies were selected. Colony identity was confirmed by Gram staining
128 and PCR using *P. intermedia*-specific primers Pi-192 and Pi-486 (Supplementary
129 Table 1). The PCR conditions were as follows: initial denaturation at 95 °C for 5 min;
130 35 cycles of 95 °C for 30 s, 55 °C for 30 s, and 72 °C for 30 s; and a final extension at
131 72 °C for 7 min.

132

133 **Cell lines and cultures**

134 The immortalized human gingival keratinocyte, Smulow–Glickman (SG) cell (17), was
135 kindly provided by Dr. Chuan-Fa Chang (NCKU) and cultured with Dulbecco's
136 Modified Eagle Medium (DMEM) (#11965-092, Gibco/Life Technology, Carisbad,
137 CA, USA). Human tongue carcinoma cell lines, SAS cells (18), and SCC-15 cells (19)
138 were obtained from Dr. Jhen-Wei Ruan (NCKU) and maintained in DMEM/F12

139 (D/F12) medium (#11330-032, Gibco). All media were supplemented with 10% FBS
140 (#10437-028, Gibco) and 1% 100x Penicillin-Streptomycin-Amphotericin B solution
141 (#CC501-0100, Simply Biotechnology, San Diego, CA, USA). Cells were incubated
142 at 37 °C in a humidified atmosphere containing 5% CO_2.
143
144 **Conditioned medium (CM) preparation**
145 The preparation of *P. intermedia* condtioned medium was adapted from a previously
146 published protocol (20). *P. intermedia* strains were anaerobically cultured in ATCC
147 2722 broth at 37 °C and were harvested when the OD600 value reached 1.0. The
148 bacterial culture was centrifuged at 3220 xg for 3 min and discarded supernatant. The
149 pellet was resuspended with a double volume of cell culture medium and anaerobically
150 incubated at 37 °C for an additional 8 hr. Then the supernatant was collected after being
151 centrifuged at 3220 xg for 10 min, filtered with a 0.22 μm filter (Merck Millipore,
152 Burlington, MA, USA), and stored at 4 °C before use.
153
154 **Cell proliferation assay**
155 The cell proliferation assay was performed as previously described (21). SG, SAS, or
156 SCC-15 cells were dissociated by 0.05% trypsin-EDTA solution (#25300-054, Gibco)
157 and resuspended in DMEM or D/F12 medium. A total of 1 x 10^4 cells were seeded into
158 each well of 24-well tissue culture plates (Corning, NY, USA) and treated with bacteria
159 or CM treatment. CM was fractionated into four components using centrifugal filter
160 devices with molecular weight cutoffs of 3 kDa, 10 kDa, and 30 kDa (Merck Millipore).
161 Treatments included 10% CM; the PAR-2 antagonist FSLLRY-NH2 at 40 μM for SG
162 cells or 20 μM for SCC-15 and SAS cells (#4751, TOCRIS/Bio-Techne, Minneapolis,
163 MN, USA); and the cysteine protease inhibitor E64 at 5 μM for SG cells or 0.5 μM for

164 SCC-15 and SAS cells (#324890, Merck Millipore). All treatments were administered
165 in DMEM or D/F12 containing 10% FBS to a final volume of 1 ml. After incubation
166 for 24, 48, or 72 hr at 37 °C in a 5% CO_2 atmosphere, cells were washed once with 1×
167 PBS and then dissociated using 0.05% trypsin-EDTA. The resulting cell suspension
168 was mixed with an equal volume of 0.4% trypan blue (#15250-061, Gibco), and viable
169 cells were counted using a Luna cell counter (Logos Biosystems, Gyeonggi-do, South
170 Korea).
171
172 **Capillary electrophoresis/Liquid Chromatography-Mass spectrometry (CE/LC**
173 **MASS) analysis**
174 A total of 100 μg of protein in 60 μl rehydration buffer (7 M urea, 2 M thiourea, and
175 2% CHAPS) was mixed with 9.3 μl of 7.5% SDS (#75746, Sigma, Burlington, MA,
176 USA) and 0.7 μl of 1 M dithiothreitol (#UR-DTT, UniRegion Bio-Tech, Taichung,
177 Taiwan) prepared in 7 M urea and 0.01 M sodium acetate. The mixture was heated at
178 95 °C for 5 min, then placed on ice for 3 min. Next, 4 μl of 500 mM IAM
179 (iodoacetamide in 50 mM ammonium bicarbonate) was added and incubated at room
180 temperature for 30 min. Afterward, 52 μl of 50% trichloroacetic acid (TCA) (#100807,
181 Merck Millipore) was added, and the solution was placed on ice for 15 min. The
182 precipitate was collected by centrifugation at 15,871 ×g for 15 min at 4 °C, resuspended
183 in 150 μl of 10% TCA, and centrifuged again at 15,871 ×g for 5 min at 4 °C. This
184 washing step was repeated three times. The final pellet was resuspended in 100 μl of
185 100 mM ammonium bicarbonate and digested with 20 μl of trypsin solution (#V5111,
186 Promega, Madison, WI, USA) at 37 °C for 16 hr. To inactivate trypsin, samples were
187 stored overnight at −80 °C. Prior to analysis, samples were desalted using Ziptips
188 (Merck Millipore). Protein identification was performed using CE/LC-MS on a Q

189 Exactive Orbitrap Mass Spectrometer (Thermo Fisher Scientific).

190

191 **Interpain A gene expression quantitative analysis (RT-qPCR)**

192 RNA extraction and RT-qPCR were adapted from previously described methods (22).
193 A 2 ml culture of *P. intermedia* (OD_{600} = 0.8) was mixed with 4 ml of RNAprotect
194 Bacteria Reagent (QIAGEN, Venlo, Netherlands). After centrifugation at 2,200 ×g for
195 5 min, the supernatant was discarded, and the pellet was stored at −80 °C until RNA
196 extraction. RNA was purified using the RNeasy Mini Kit (QIAGEN), and residual
197 DNA was removed using DNase (Promega). The resulting RNA was concentrated with
198 the Clean & Concentrator Kit (ZYMO GENETICS, Seattle, WA, USA). cDNA was
199 synthesized from the RNA using the SuperScript III First-Strand System with random
200 hexamers (Invitrogen, Waltham, MA, USA). RT-qPCR was performed using GoTaq
201 qPCR Master Mix (Promega) on a MyGo Pro real-time PCR instrument (IT-IS Life
202 Science Ltd/DKSH, St Leonards, Australia) with primers inpA F, inpA R, Pi 16S rRNA
203 F, and Pi 16S rRNA R (Supplementary Table 1). The thermal cycling conditions were
204 as follows: initial denaturation at 95 °C for 10 min, followed by 40 cycles of
205 denaturation at 95 °C for 15 s and annealing/extension at 60 °C for 1 min. A melt curve
206 analysis was performed from 60 to 97 °C at a ramp rate of 0.1 °C/s. All procedures
207 were conducted in accordance with the manufacturers' instructions.

208

209 **$InpA_{N381}$ expression vector construction and recombinant $InpA_{N381}$ purification**

210 Genomic DNA of *P. intermedia* ATCC 25611 was extracted using the MasterPure^{TM}
211 complete DNA and RNA purification kit (Lucigen Corp, Middleton, WI, USA)
212 according to the manufacturer's instructions. The gene region encoding the signal
213 peptide, pro-domain, and catalytic domain ($inpA_{N381}$) was amplified using a mixture of

214 GoTaq G2 Flexi DNA Polymerase (Promega) and Pfu polymerase (Promega) with
215 primers *inpA*$_{N381}$ F and *inpA*$_{N381}$ R (Supplementary Table1). The PCR product was
216 digested with BamHI and XhoI and ligated into the pET21b(+) expression vector pre-
217 digested with the same enzymes. The resulting plasmid, pET21b(+)::*inpA*$_{N381}$, was
218 verified by sequencing and chemically transformed into *Escherichia coli* C41 (DE3)
219 cells. A single colony of *E. coli* C41 (DE3) harboring pET21b(+)::*inpA*$_{N381}$ was
220 inoculated into 20 ml LB broth supplemented with ampicillin (100 μg/ml) and cultured
221 at 37 °C for 14-16 hr with shaking at 170 rpm. The bacterial culture was then refreshed
222 with 2 liters LB at the ratio of 1:100 and grew at 37 °C with shaking at 170 rpm until
223 OD600 reached 0.4. Protein expression was induced by adding 0.2 mM isopropyl-β-
224 D-thiogalactoside (IPTG; #101-367-93-1, Cyrusbioscience, Inc., Seattle, WA, USA),
225 followed by incubation at 25 °C for an additional 16 hr with shaking (23). After
226 induction, the bacterial culture was centrifuged at 3,300 ×g for 40 min at 4 °C. The
227 resulting pellet was resuspended in 100 ml of 1× PBS and lysed by ultrasonication on
228 ice (20 s pulse on, 100 s pulse off) until complete cell disruption. The lysate was then
229 centrifuged at 16,000 ×g for 40 min at 4 °C. InpA$_{N381}$ protein was purified from the
230 supernatant using a HisTrap HP His-tag affinity column (Cytiva, Washington D.C.,
231 USA) according to the manufacturer's instructions. The purified InpA$_{N381}$ protein was
232 washed with 100 volumes of 1× PBS and stored at −20 °C until use.
233
234 **Transwell assay**
235 The Transwell assay was conducted as previously described (24). SAS or SCC-15 cells
236 were resuspended in D/F12 medium supplemented with 10% FBS. Cell concentration
237 was adjusted to 1 × 10^5 cells/ml. A total of 100 μl of cell suspension was added to the
238 upper chamber of Transwell inserts (8 μm pore size, Falcon/Corning, NY, USA) placed

239 in a 24-well plate and incubated at 37 °C in 5% CO_2. The lower chamber was filled
240 with 10% CM, 20 μM FSLLRY-NH_2, or 0.5 μM E64, in D/F12 containing 10% FBS,
241 to a final volume of 600 μl. After 24 hr, cells in the upper chamber were removed with
242 cotton swabs, and migrated cells on the lower side of the membrane were fixed with
243 70% ethanol for 10 min and stained with 0.2% crystal violet for 5 min. Five random
244 fields per membrane were selected for cell counting under an inverted microscope
245 (Leica Microsystems, Wetzlar, Germany).
246
247 **Wound healing assay**
248 The wound healing assay was performed according to a previously reported method
249 (24). SAS or SCC-15 cells were seeded in both compartments of each block insert (SPL
250 Life Sciences Co., Gyeonggi-do, Korea), placed in 24-well plates, and incubated at
251 37 °C with 5% CO_2 for 24 hr. The inserts were then removed, and the wells were
252 washed once with 1× PBS. Cells were treated with 10% CM, 20 μM FSLLRY-NH_2, or
253 0.5 μM E64, with the total volume adjusted to 1 ml using D/F12 containing 10% FBS.
254 Images were captured every 2 hr using a microscope (OLYMPUS, Tokyo, Japan) to
255 monitor gap closure. Gap widths were measured using ImageJ, and wound closure rates
256 were calculated by dividing the change in width over time.
257
258 **Colorectal cancer (CRC) mouse model**
259 The mouse model was modified from previously published protocols (25). Seven-
260 week-old specific pathogen-free (SPF) male C57BL/6 mice were purchased from the
261 Laboratory Animal Center of NCKU. Mice received a single intraperitoneal injection
262 of azoxymethane (AOM; Sigma-Aldrich) at 12.5 mg/kg, followed by administration of
263 2% dextran sodium sulfate (DSS; MP Biomedicals, Irvine, CA, USA) in drinking water

264 to induce colorectal cancer. Twenty mice were randomly assigned to four groups:
265 MOCK, AOM/DSS, AOM/DSS + *F. nucleatum*, and AOM/DSS + *P. intermedia*. Mice
266 underwent three cycles of DSS and bacterial treatment. Each cycle lasted 3 weeks: 5
267 days of 2% DSS in the first week, followed by two weeks of oral gavage with either
268 1× PBS or 1×10^9 CFU of *F. nucleatum* (ATCC 23726) or *P. intermedia* (ATCC 25611)
269 once per week. Mice were sacrificed at week 10, and colons were harvested,
270 longitudinally opened, and tumor numbers were counted.
271
272 **Statistical analysis**
273 Statistical analyses were conducted using GraphPad Prism 8 software. All data were
274 obtained from experiments performed in triplicate. Comparisons between two groups
275 were assessed using the Student's t-test, while multiple group comparisons were
276 analyzed by one-way ANOVA. Statistical significance was indicated as follows: $p <$
277 0.05 (*), $p < 0.01$ (**), $p < 0.001$ (***), and $p < 0.0001$ (****).
278
279 ## Results
280 ***P. intermedia* ATCC 25611 enhances human oral cell proliferation**
281 A previous study at National Cheng Kung University Hospital (NCKUH)
282 reported a significant increase in *P. intermedia* abundance in patients with oral
283 squamous cell carcinoma (OSCC) compared to healthy controls (6). To investigate the
284 potential contribution of *P. intermedia* to OSCC development, we assessed its effect
285 on oral epithelial cell proliferation. The reference strain ATCC 25611 was tested at
286 multiple multiplicities of infection (MOIs) using the human normal oral epithelial cell
287 line SG. After 24 hours of co-culture, *P. intermedia* ATCC 25611 significantly
288 increased SG cell numbers at an MOI of 100 compared to the uninfected control group

289 (Fig. 1A, 1B). In addition to ATCC 25611, we also examined six clinical isolates of
290 *P. intermedia* obtained from patient saliva samples at NCKUH. Among these, strains
291 H26219-3, H29383, and H29703 were isolated from OSCC patients, while strains
292 H31082, H29823, and H31226 were obtained from individuals with non-cancerous oral
293 conditions. SG cells were co-cultured with each clinical isolate at MOI 100. Unlike
294 ATCC 25611, these strains did not induce a proliferation increase in SG cells; notably,
295 strain H29383 even reduced SG cell numbers after 24 hours (Fig. 1B; Fig. S1A). We
296 further found that only live *P. intermedia* was capable of promoting SG cell
297 proliferation (Fig. 1C), likely due to its limited viability under aerobic conditions,
298 which may confine its activity to the early co-culture period. Similarly, conditioned
299 medium (CM) from strain ATCC 25611 increased SG cell proliferation, whereas CM
300 from the clinical strains failed to elicit the same response (Fig. 1D; Fig. S1B). These
301 findings were corroborated using EdU incorporation assays (Fig. S1C), which supports
302 the role of a secreted factor in enhancing proliferation. To identify this active factor,
303 we subjected the CM to heat inactivation, which abolished its proliferative effect (Fig.
304 1D), indicating the involvement of a heat-sensitive, likely proteinaceous molecule.
305 Further size-fractionation of CM revealed that only the >30 kDa fraction retained
306 stimulatory activity (Fig. 1E). Additionally, CM from ATCC 25611 significantly
307 enhanced proliferation in OSCC cell lines SCC-15 and SAS after 48 and 72 hours,
308 respectively (Fig. 1F, 1G), suggesting that *P. intermedia* promotes oral epithelial cell
309 proliferation through the action of one or more secreted proteins.
310
311 **Interpain A plays a centrol role in *P. intermedia* ATCC 25611 promoting oral cell**
312 **proliferation**

313 Following our observation that strain ATCC 25611 and several clinical isolates
314 exhibited divergent effects on SG cell proliferation, we hypothesized that these
315 differences could be attributed to the expression of specific secreted protein(s). To
316 investigate this, we conducted proteomic analysis of conditioned medium (CM) from
317 strain ATCC 25611 and the non-proliferative strain H31226 using capillary
318 electrophoresis/liquid chromatography-mass spectrometry (CE/LC-MS). Several
319 proteins were found to be more abundant in the CM of ATCC 25611 compared to that
320 of H31226 (Supplementary Table 2). Among these, interpain A (InpA), a secreted
321 cysteine protease, was particularly enriched—present at levels thirteen times higher in
322 ATCC 25611 than in H31226 (Fig. 2A). InpA is a 90 kDa cysteine protease previously
323 reported to facilitate heme acquisition for bacterial growth and to degrade complement
324 factor C3, aiding immune evasion (26-28). Notably, *P. gingivalis*, another oral
325 anaerobe strongly associated with chronic periodontitis and cancer, produces similar
326 cysteine proteases called gingipains, which have been shown to activate protease-
327 activated receptors (PARs) on oral epithelial cells (11). Gingipains, in particular, have
328 been implicated in OSCC progression through activation of PAR-2 signaling,
329 enhancing cell migration and invasiveness (29, 30). Given these functional similarities,
330 we hypothesized that InpA may enhance oral epithelial cell proliferation via activation
331 of the PAR-2 signaling pathway. To test this hypothesis, SG cells were treated with
332 CM from ATCC 25611 in the presence of either E64, a cysteine protease inhibitor, or
333 FSLLRY-NH_2, a PAR-2 antagonist. After 24 hours, the proliferation-promoting effects
334 of CM were significantly attenuated by both inhibitors (Fig. 2B). A similar inhibition
335 pattern was observed under direct bacterial co-culture conditions. These results were
336 consistent across SCC-15 and SAS oral cancer cell lines, where the proliferative effects
337 observed after 48 hours were also blocked by E64 or FSLLRY-NH_2 treatment (Fig. 2C,

338 2D). To further confirm InpA's direct effect, we expressed and purified the
339 recombinant catalytic domain of InpA ($InpA_{N381}$) in *E. coli* strain C41. $InpA_{N381}$
340 stimulated SCC-15 proliferation in a manner consistent with that of native CM, and
341 again, this effect was neutralized by either E64 or FSLLRY-NH_2 treatment (Fig. 2E).
342 Importantly, treatment with E64 or FSLLRY-NH_2 alone had no effect on the
343 proliferation of SG, SCC-15, or SAS cells (Fig. S2), confirming that the inhibitors'
344 effects were specific to the activity of InpA or the associated pathway. We next
345 investigated whether differences in InpA production could explain the observed strain-
346 dependent variability in proliferation. RT-qPCR analysis revealed significantly higher
347 *inpA* expression in ATCC 25611 compared to all clinical isolates tested (Fig. 2F).
348 Furthermore, among the clinical strains, those isolated from OSCC patients (H26219-
349 3, H29383, and H29703) exhibited higher *inpA* expression than strains from patients
350 with non-cancerous oral diseases (H31082, H29823, and H31226). These findings
351 collectively indicate that *P. intermedia* promotes oral epithelial cell proliferation via
352 InpA and the PAR-2 signaling axis and that this activity is strain-dependent, correlating
353 with InpA production levels.
354

355 **InpA-Mediated Promotion of OSCC Cell Migration**

356 During cancer progression, tumor cells initially undergo uncontrolled growth
357 at the primary site, followed by invasion and dissemination to distant organs—a
358 process known as metastasis. Metastasis involves the degradation of the extracellular
359 matrix, intravasation into the vasculature, and colonization of secondary tissues, and is
360 a major contributor to cancer-related mortality (31). Given our findings that *P.*
361 *intermedia* promotes oral epithelial cell proliferation, we next investigated whether it
362 also influences OSCC cell migration. To address this, we employed two

363 complementary assays—wound healing and transwell migration assays—using SCC-
364 15 and SAS OSCC cell lines. In the wound healing assay, treatment with conditioned
365 medium (CM) from *P. intermedia* strain ATCC 25611 significantly enhanced the
366 migration rate of both cell lines at 2 and 4 hours post-treatment compared to untreated
367 controls (Fig. 3A, 3B). To determine whether this migration-promoting effect involved
368 InpA and PAR-2 signaling, we co-treated cells with either E64 or FSLLRY-NH_2. Both
369 inhibitors effectively abrogated the CM-induced enhancement of cell migration.
370 Similarly, in the transwell migration assay, CM from ATCC 25611 significantly
371 increased the number of migrating SCC-15 and SAS cells after 24 hours (Fig. 3C, 3D).
372 Treatment with E64 or FSLLRY-NH_2 had no significant effect on SCC-15 and SAS
373 cell migration in either wound healing or transwell assays (Fig. S3). Co-treatment with
374 E64 or FSLLRY-NH_2 suppressed this enhanced migratory response. Furthermore,
375 recombinant $InpA_{N381}$ purified from *E. coli* elevated SCC-15 cell migration (Fig. 3E),
376 and this effect was also blocked by both E64 and FSLLRY-NH_2. Together, these
377 findings suggest that *P. intermedia* facilitates OSCC cell migration through an InpA-
378 dependent mechanism involving PAR-2 signaling, paralleling its role in cell
379 proliferation.
380
381 ***P. intermedia* increases tumor burden in a colorectal cancer mouse model**
382 An increasing body of evidence suggests that oral microbiota not only
383 contributes to oral diseases but also plays a role in systemic conditions such as cystic
384 fibrosis, cardiovascular disease, rheumatoid arthritis, and gastrointestinal disorders
385 (32). Furthermore, several oral bacteria have been linked to cancers in distal organs,
386 including the pancreas, breast, stomach, esophagus, and colon (32). The concept of the
387 oral-gut axis proposes that oral bacteria can translocate to the gastrointestinal tract,

388 where they may disrupt the gut microbial balance and contribute to diseases such as
389 inflammatory bowel disease and colorectal cancer (CRC) (33, 34). Notably,
390 *Fusobacterium nucleatum*, an oral anaerobe, has been identified as an important
391 contributor to CRC progression (35). Given the pro-tumorigenic effects of *P.*
392 *intermedia* observed in OSCC, we hypothesized that it may also influence CRC
393 development. To test this, we used an azoxymethane (AOM) and 2% dextran sulfate
394 sodium (DSS)-induced CRC model in C57BL/6 mice, followed by oral gavage with
395 either *F. nucleatum* or *P. intermedia*. Compared to the AOM/DSS-only group, both
396 bacterial treatments significantly increased tumor formation and elevated the number
397 of colonic tumors (Fig. 4B, 4C). These results suggest that *P. intermedia*, like *F.*
398 *nucleatum*, may contribute to CRC pathogenesis and should be considered a relevant
399 microbial factor in colorectal tumorigenesis.
400

401 **Discussion**

402 The present study demonstrated that *P. intermedia* may play a significant role in
403 oral cancer development. Interpain A (InpA), a cysteine protease secreted by *P.*
404 *intermedia*, functioned as an effector that enhanced both oral epithelial cell
405 proliferation (Fig. 2B) and OSCC cell migration (Fig. 3A–D). Importantly, these
406 effects were linked to the protease-activated receptor-2 (PAR-2) signaling pathway
407 activation. Prior studies examining salivary samples from OSCC patients reported
408 increased expression of various oral bacterial virulence genes, including *fadA* and *inpA*
409 (36). Notably, PAR-2 has been implicated in promoting cell proliferation, metastasis,
410 and invasion in multiple cancers, including OSCC, esophageal carcinoma, and
411 pancreatic cancer (37). Previous studies have also shown that gingipains, secreted
412 cysteine proteases from *P. gingivalis*, can activate the PAR-2/NF-κB signaling axis and

413 induce proMMP9 expression, thereby facilitating OSCC invasion (11). These findings
414 are consistent with our observations implicating InpA and PAR-2 signaling in OSCC
415 progression.

416 Our results showed that *P. intermedia*-CM treatment promoted proliferation in
417 both normal oral keratinocytes (SG cells) and OSCC cell lines (SCC-15 and SAS) (Fig.
418 1D–G). Interestingly, the proliferative effect manifested at different time points
419 between cell types: SG cells responded within 24 hours, whereas SCC-15 and SAS
420 cells showed continued stimulation at 48 and 72 hours. Moreover, SG cell numbers
421 decreased after 48 hours, suggesting that normal oral cells may retain mechanisms to
422 counterbalance proliferative signals, while cancer cells have lost this regulatory
423 capacity. A previous study of *P. gingivalis* reported G_1 cell cycle arrest and apoptosis
424 in trophoblasts, as well as in osteoblastic/stromal cells following gingipain exposure
425 (38, 39). Gingipains have also been shown to induce apoptosis in oral epithelial cells
426 (40). It is possible that InpA exerts similar effects in SG cells following initial
427 proliferation, potentially through the regulation of cell cycle or apoptotic pathways.
428 This observation warrants further investigation. Our findings also highlight the need to
429 clarify whether InpA differentially activates downstream PAR-2 signaling in normal
430 versus malignant oral cells.

431 The concept of an oral-gut microbiome axis is increasingly supported by
432 evidence showing that oral dysbiosis can influence both local and systemic health (41);
433 A growing number of studies have linked oral microbiota imbalances with
434 gastrointestinal diseases, including colorectal cancer (CRC) (42). Recent findings
435 suggest that *P. intermedia* enhances CRC cell proliferation and migration through
436 secreted protein effectors, similar to those identified in our OSCC model (43). The
437 promoting effect was also from *P. intermedia*-secreted protein(s). Those results were

438 similar to our findings (Fig. 2C-E). In agreement with these findings, our data showed
439 that oral administration of *P. intermedia* increased tumor burden in an AOM/DSS-
440 induced CRC mouse model (Fig. 4). These results reinforce the idea that *P. intermedia*
441 may act as a tumor-promoting microbe across multiple tissue contexts. Beyond cancer,
442 *P. intermedia* and other oral pathogens have been implicated in the pathogenesis of
443 various systemic diseases (44). Oral bacteria are capable of releasing inflammatory
444 mediators that may affect the central nervous system. Elevated serum antibody levels
445 against *P. gingivalis*, *F. nucleatum,* and *P. intermedia* have been observed in patients
446 with Alzheimer's disease (45). Gingipains from *P. gingivalis* have been detected in the
447 brains of Alzheimer's patients and are known to increase blood–brain barrier
448 permeability (8, 46). Moreover, gingipains have been associated with other
449 neurodegenerative diseases, such as Parkinson's disease (47). Periodontal bacteria
450 have also been identified in atheromatous plaques and are believed to contribute to
451 cardiovascular disease pathogenesis (48, 49). These findings position *P. intermedia* as
452 a potentially important contributor to systemic inflammatory and degenerative diseases.
453 Our study also supports the notion that the pro-proliferative effects of *P.*
454 *intermedia* are strain-dependent. In SG cells, only strain ATCC 25611 induced
455 proliferation at MOI 100 (Fig. 1B, S1A), and only its conditioned medium promoted
456 proliferation (Fig. 1D, S1B). Proteomic analysis confirmed that this strain secreted
457 significantly higher levels of InpA than clinical isolates such as H31226 (Fig. 2A), and
458 RT-qPCR revealed higher *inpA* expression in strains isolated from OSCC patients
459 compared to non-cancer controls (Fig. 2F). These observations raise the possibility of
460 using salivary InpA levels as a biomarker for OSCC risk or diagnosis. Although there
461 was no statistically significant difference between clinical strain H26219-3 or H29383
462 and the untreated control group at the 24-hour time point (Fig. S1B), SG cell

463 proliferation showed a mild upward trend in response to both strains isolated from
464 OSCC patients. This observation suggests that these strains may exert weak but
465 measurable biological effects. Given that such bacteria can persistently colonize the
466 oral cavity, it is plausible that their cumulative impact over time could become
467 biologically relevant. However, short-term cell-based assays are unlikely to capture
468 such long-term effects.

469 To explore the mechanism underlying InpA-dependent proliferation, we
470 performed a Micro-Western Array focusing on signaling pathways related to cell
471 growth in SG cells (Fig. S4). We found that the EGFR signaling pathway was
472 upregulated, with RAF expression increasing at 8 hours and decreasing at 24 hours.
473 This aligns with prior studies showing that the EGFR–RAS–RAF–MEK–ERK axis is
474 frequently upregulated in OSCC (50). While these findings provide a preliminary
475 mechanistic link between InpA and cancer signaling pathways, further validation is
476 required.

477 In conclusion, our study demonstrates that InpA, a cysteine protease secreted by
478 *P. intermedia*, plays a pivotal role in promoting oral epithelial cell proliferation and
479 OSCC cell migration. These effects appear to be mediated via the PAR-2 signaling
480 pathway and are strain-dependent. The results suggest a potential microbial mechanism
481 contributing to OSCC development and lay the groundwork for future investigations
482 into therapeutic strategies targeting microbial virulence factors.

483

484 **Figure legends**

485 **Figure 1. *P. intermedia* ATCC 25611 enhances proliferation of normal and**
486 **cancerous oral epithelial cells.** (A) Human normal oral epithelial SG cells were
487 infected with live *P. intermedia* strain ATCC 25611 at a multiplicity of infection (MOI)

488 of 100 or 1000 for 24 or 48 hours. (B) SG cells were co-cultured with strain ATCC
489 25611 or clinical isolates H29383 and H31226 at MOI 100. (C) Comparison of live
490 versus UV-inactivated *P. intermedia* strain ATCC 25611 on SG cell proliferation. (D)
491 Proliferative effect of conditioned medium (CM) from ATCC 25611 versus heat-
492 inactivated CM on SG cells. (E) CM of strain ATCC 25611 was fractionated by
493 molecular weight using centrifugal filters: >30 kDa, 10–30 kDa, 3–10 kDa, and <3 kDa.
494 (F–G) CM from ATCC 25611 was applied to oral squamous carcinoma cell lines SCC-
495 15 and SAS for 24, 48, and 72 hours. All results are representative of three independent
496 experiments. Data are shown as mean ± SD. Statistical analysis was performed by one-
497 way ANOVA (A–C) or t-test (D). ns: not significant; *$p < 0.05$; **$p < 0.01$; ***$p <$
498 0.001; ****$p < 0.0001$.
499
500 **Figure 2. InpA promotes oral cell proliferation via PAR-2 activation.** (A) CE/LC-
501 MS identified elevated levels of InpA in strain ATCC 25611 compared to clinical strain
502 H31226, which did not stimulate SG cell proliferation. (B) SG cell proliferation in
503 response to CM or live *P. intermedia* (MOI 100), with or without 5 μM E64 (protease
504 inhibitor) or 40 μM FSLLRY-NH_2 (PAR-2 antagonist). (C-D) SCC-15 and SAS cell
505 proliferation following treatment with CM from ATCC 25611, with or without 0.5 μM
506 E64 or 20 μM FSLLRY-NH_2. (E) Five micrograms of recombinant InpA (rInpA) were
507 applied to SCC-15 cells, with or without E64 or FSLLRY-NH_2. PBS served as a vehicle
508 control; CM from ATCC 25611 served as a positive control. (F) Quantitative RT-PCR
509 analysis of *inpA* gene expression in ATCC 25611 and six clinical isolates. Strains
510 H26219-3, H29383, and H29703 were from oral cancer patients (CA), while H31082,
511 H29823, and H31226 were from control patients (CO). Expression levels were
512 calculated using the 2^–ΔΔCt method.

513 All results are representative of three independent experiments. Data are expressed as
514 mean ± SD and analyzed by one-way ANOVA. ns: not significant; *$p < 0.05$; ****$p <$
515 0.0001.
516
517 **Figure 3. InpA enhances OSCC cell migration through PAR-2 signaling.** (A–B)
518 Wound healing assays in SCC-15 (A) and SAS (B) cells treated with standard medium
519 (D/F12), CM from ATCC 25611, or CM with 0.5 μM E64 or 20 μM FSLLRY-NH_2.
520 Cell migration was assessed at 2 and 4 hours and calculated as migration rate (μm/hr).
521 (C–D) Transwell migration assays in SCC-15 (C) and SAS (D) cells treated as above
522 for 24 hours. Migrated cells were quantified under a phase-contrast microscope. (E)
523 Transwell migration of SCC-15 cells treated with 5 μg/mL recombinant InpA (rInpA)
524 with or without E64 or FSLLRY-NH_2. All data represent triplicate experiments and are
525 shown as mean ± SD. One-way ANOVA was used for statistical analysis. ns: not
526 significant; **$p < 0.01$; ***$p < 0.001$; ****$p < 0.0001$.
527
528 **Figure 4. Oral administration of *P. intermedia* increases colorectal tumor burden**
529 **in mice.** (A) Schematic diagram of the azoxymethane (AOM)/dextran sulfate sodium
530 (DSS)-induced colorectal cancer (CRC) mouse model. Mice received a single
531 intraperitoneal injection of AOM (12.5 mg/kg), followed by three cycles of 2% DSS
532 in drinking water (5 days per cycle, separated by 16 days of regular water). During the
533 DSS cycles, 1×10^9 CFU of *P. intermedia* ATCC 25611 or *F. nucleatum* ATCC 23726
534 was administered via oral gavage. Mice were euthanized at week 10. (B)
535 Representative images of distal colon morphology from AOM/DSS mice with or
536 without bacterial infection. (C) Quantification of tumor number in the distal colon.
537 Each group included five mice. ns: not significant; *$p < 0.05$.

Acknowledgements. We thank the Laboratory Animal Center, College of Medicine at National Cheng Kung University (NCKU), Taiwan, accredited by AAALAC International and Taiwan Animal Consortium, for their support in caring for mice. We appreciate the participation of all patients in this study. We are grateful to all the unmentioned clinicians and recruiters. We also thank Dr. Chuan-Fa Chang and Dr. Jhen-Wei Ruan provided the cell lines.

Financial support: This work was supported by the National Science and Technology Council (Grants: 113-2314-B-006-043-MY3) awarded to J. W. C. and OSU-CHS Startup awarded to I.H.H.. The funding agencies played no role in study design, data collection or analysis, manuscript preparation, or decision to publish.

Authors' contributions: S.-M. C., Y.-J. C., W.-R. W. and N.-H. W. performed the experiments. S.-M. C. wrote this manuscript. I-H. H. assisted with the experimental design and reviewed this manuscript. C.-P. C. performed the microwestern array experiments and reviewed this manuscript. J.-R. H., J. S C., and J.-Y. C. provided clinical patients' saliva. J.-W. C. contributed to design, provide the concept, and supervise this manuscript. All authors have read and approved the final version of this manuscript.

References:

1. Jhuang JR, Su SY, Chiang CJ, Yang YW, Lin LJ, Hsu TH, et al. Forecast of peak attainment and imminent decline after 2017 of oral cancer incidence in men in Taiwan. Sci Rep. 2022;12(1):5726.
2. Tuominen H, Rautava J. Oral Microbiota and Cancer Development. Pathobiology. 2021;88(2):116-26.
3. Zhang L, Liu Y, Zheng HJ, Zhang CP. The Oral Microbiota May Have Influence on Oral Cancer. Front Cell Infect Microbiol. 2019;9:476.
4. Karmakar S, Kar A, Thakur S, Rao VUS. Periodontitis and oral Cancer-A striking link. Oral Oncology. 2020;106:104630.
5. Kirst ME, Li EC, Alfant B, Chi Y-Y, Walker C, Magnusson I, et al. Dysbiosis

568 and alterations in predicted functions of the subgingival microbiome in chronic
569 periodontitis. Appl Environ Microbiol. 2015;81(2):783-93.
570 6. Hsiao JR, Chang CC, Lee WT, Huang CC, Ou CY, Tsai ST, et al. The
571 interplay between oral microbiome, lifestyle factors and genetic polymorphisms in
572 the risk of oral squamous cell carcinoma. Carcinogenesis. 2018;39(6):778-87.
573 7. Chattopadhyay I, Verma M, Panda M. Role of Oral Microbiome Signatures in
574 Diagnosis and Prognosis of Oral Cancer. Technol Cancer Res Treat.
575 2019;18:1533033819867354.
576 8. Dominy SS, Lynch C, Ermini F, Benedyk M, Marczyk A, Konradi A, et al.
577 Porphyromonas gingivalis in Alzheimer's disease brains: Evidence for disease
578 causation and treatment with small-molecule inhibitors. Sci Adv.
579 2019;5(1):eaau3333.
580 9. Wen L, Mu W, Lu H, Wang X, Fang J, Jia Y, et al. Porphyromonas gingivalis
581 Promotes Oral Squamous Cell Carcinoma Progression in an Immune
582 Microenvironment. Journal of Dental Research. 2020;99(6):666-75.
583 10. Liu Y, Yuan X, Chen K, Zhou F, Yang H, Yang H, et al. Clinical significance
584 and prognostic value of Porphyromonas gingivalis infection in lung cancer. Transl
585 Oncol. 2021;14(1):100972.
586 11. Inaba H, Sugita H, Kuboniwa M, Iwai S, Hamada M, Noda T, et al.
587 Porphyromonas gingivalis promotes invasion of oral squamous cell carcinoma
588 through induction of proMMP9 and its activation. Cell Microbiol. 2014;16(1):131-
589 45.
590 12. Geng F, Zhang Y, Lu Z, Zhang S, Pan Y. Fusobacterium nucleatum Caused
591 DNA Damage and Promoted Cell Proliferation by the Ku70/p53 Pathway in Oral
592 Cancer Cells. DNA Cell Biol. 2020;39(1):144-51.
593 13. Parhi L, Alon-Maimon T, Sol A, Nejman D, Shhadeh A, Fainsod-Levi T, et
594 al. Breast cancer colonization by Fusobacterium nucleatum accelerates tumor growth
595 and metastatic progression. Nature Communications. 2020;11(1):3259.
596 14. Rubinstein MR, Wang X, Liu W, Hao Y, Cai G, Han YW. Fusobacterium
597 nucleatum promotes colorectal carcinogenesis by modulating E-cadherin/β-catenin
598 signaling via its FadA adhesin. Cell Host Microbe. 2013;14(2):195-206.
599 15. Gur C, Ibrahim Y, Isaacson B, Yamin R, Abed J, Gamliel M, et al. Binding of
600 the Fap2 protein of Fusobacterium nucleatum to human inhibitory receptor TIGIT
601 protects tumors from immune cell attack. Immunity. 2015;42(2):344-55.
602 16. Tompkins GR, Wood DP, Birchmeier KR. Detection and comparison of
603 specific hemin binding by Porphyromonas gingivalis and Prevotella intermedia. J
604 Bacteriol. 1997;179(3):620-6.
605 17. Babich H, Tipton DA. In vitro response of human gingival epithelioid S-G
606 cells to minocycline. Toxicol In Vitro. 2002;16(1):11-21.
607 18. TAKAHASHI K, KANAZAWA H, AKIYAMA Y, TAZAKI S,
608 TAKAHARA M, MUTO T, et al. Establishment and characterization of a cell
609 line(SAS) from poorly differentiated human squamous cell carcinoma of the tongue.
610 Journal of The Japanese Stomatological Society. 1989;38(1):20-8.
611 19. Rheinwald JG, Beckett MA. Tumorigenic keratinocyte lines requiring
612 anchorage and fibroblast support cultured from human squamous cell carcinomas.
613 Cancer research. 1981;41 5:1657-63.
614 20. Scheres N, de Vries TJ, Brunner J, Crielaard W, Laine ML, Everts V. Diverse
615 effects of Porphyromonas gingivalis on human osteoclast formation. Microb Pathog.
616 2011;51(3):149-55.
617 21. Yang Y, Weng W, Peng J, Hong L, Yang L, Toiyama Y, et al. Fusobacterium

618 nucleatum Increases Proliferation of Colorectal Cancer Cells and Tumor
619 Development in Mice by Activating Toll-Like Receptor 4 Signaling to Nuclear
620 Factor-κB, and Up-regulating Expression of MicroRNA-21. Gastroenterology.
621 2017;152(4):851-66.e24.
622 22. Chen KY, Rathod J, Chiu YC, Chen JW, Tsai PJ, Huang IH. The
623 Transcriptional Regulator Lrp Contributes to Toxin Expression, Sporulation, and
624 Swimming Motility in Clostridium difficile. Front Cell Infect Microbiol. 2019;9:356.
625 23. Wang ST, Kuo CJ, Huang CW, Lee TM, Chen JW, Chen CS. OmpR
626 coordinates the expression of virulence factors of Enterohemorrhagic Escherichia coli
627 in the alimentary tract of Caenorhabditis elegans. Mol Microbiol. 2021;116(1):168-
628 83.
629 24. Justus CR, Marie MA, Sanderlin EJ, Yang LV. Transwell In Vitro Cell
630 Migration and Invasion Assays. Methods Mol Biol. 2023;2644:349-59.
631 25. Yu MR, Kim HJ, Park HR. Fusobacterium nucleatum Accelerates the
632 Progression of Colitis-Associated Colorectal Cancer by Promoting EMT. Cancers
633 (Basel). 2020;12(10).
634 26. Mallorquí-Fernández N, Manandhar SP, Mallorquí-Fernández G, Usón I,
635 Wawrzonek K, Kantyka T, et al. A new autocatalytic activation mechanism for
636 cysteine proteases revealed by Prevotella intermedia interpain A. J Biol Chem.
637 2008;283(5):2871-82.
638 27. Potempa M, Potempa J, Kantyka T, Nguyen KA, Wawrzonek K, Manandhar
639 SP, et al. Interpain A, a cysteine proteinase from Prevotella intermedia, inhibits
640 complement by degrading complement factor C3. PLoS Pathog. 2009;5(2):e1000316.
641 28. Byrne DP, Wawrzonek K, Jaworska A, Birss AJ, Potempa J, Smalley JW.
642 Role of the cysteine protease interpain A of Prevotella intermedia in breakdown and
643 release of haem from haemoglobin. Biochem J. 2009;425(1):257-64.
644 29. Liu Y, Wu Z, Nakanishi Y, Ni J, Hayashi Y, Takayama F, et al. Infection of
645 microglia with Porphyromonas gingivalis promotes cell migration and an
646 inflammatory response through the gingipain-mediated activation of protease-
647 activated receptor-2 in mice. Sci Rep. 2017;7(1):11759.
648 30. Nonaka S, Nakanishi H. Secreted gingipains from Porphyromonas gingivalis
649 induce microglia migration through endosomal signaling by protease-activated
650 receptor 2. Neurochem Int. 2020;140:104840.
651 31. Chaffer CL, Weinberg RA. A perspective on cancer cell metastasis. Science.
652 2011;331(6024):1559-64.
653 32. Peng X, Cheng L, You Y, Tang C, Ren B, Li Y, et al. Oral microbiota in
654 human systematic diseases. International Journal of Oral Science. 2022;14(1):14.
655 33. Read E, Curtis MA, Neves JF. The role of oral bacteria in inflammatory
656 bowel disease. Nature Reviews Gastroenterology & Hepatology. 2021;18(10):731-
657 42.
658 34. Kudra A, Muszyński D, Sobocki BK, Atzeni A, Carbone L, Kaźmierczak-
659 Siedlecka K, et al. Insights into oral microbiome and colorectal cancer - on the way
660 of searching new perspectives. Front Cell Infect Microbiol. 2023;13:1159822.
661 35. Wu N, Feng YQ, Lyu N, Wang D, Yu WD, Hu YF. Fusobacterium nucleatum
662 promotes colon cancer progression by changing the mucosal microbiota and colon
663 transcriptome in a mouse model. World J Gastroenterol. 2022;28(18):1981-95.
664 36. Moghimi M, Bakhtiari R, Mehrabadi JF, Jamshidi N, Jamshidi N,
665 Siyadatpanah A, et al. Interaction of human oral cancer and the expression of
666 virulence genes of dental pathogenic bacteria. Microb Pathog. 2020;149:104464.
667 37. Sheng J, Deng X, Zhang Q, Liu H, Wang N, Liu Z, et al. PAR-2 promotes

invasion and migration of esophageal cancer cells by activating MEK/ERK and PI3K/Akt signaling pathway. Int J Clin Exp Pathol. 2019;12(3):787-97.
38. Inaba H, Kuboniwa M, Sugita H, Lamont RJ, Amano A. Identification of signaling pathways mediating cell cycle arrest and apoptosis induced by Porphyromonas gingivalis in human trophoblasts. Infect Immun. 2012;80(8):2847-57.
39. Kato T, Tsuda T, Inaba H, Kawai S, Okahashi N, Shibata Y, et al. Porphyromonas gingivalis gingipains cause G(1) arrest in osteoblastic/stromal cells. Oral Microbiol Immunol. 2008;23(2):158-64.
40. Stathopoulou PG, Galicia JC, Benakanakere MR, Garcia CA, Potempa J, Kinane DF. Porphyromonas gingivalis induce apoptosis in human gingival epithelial cells through a gingipain-dependent mechanism. BMC Microbiol. 2009;9:107.
41. Park SY, Hwang BO, Lim M, Ok SH, Lee SK, Chun KS, et al. Oral-Gut Microbiome Axis in Gastrointestinal Disease and Cancer. Cancers (Basel). 2021;13(9).
42. Zhang S, Kong C, Yang Y, Cai S, Li X, Cai G, et al. Human oral microbiome dysbiosis as a novel non-invasive biomarker in detection of colorectal cancer. Theranostics. 2020;10(25):11595-606.
43. Lo CH, Wu DC, Jao SW, Wu CC, Lin CY, Chuang CH, et al. Enrichment of Prevotella intermedia in human colorectal cancer and its additive effects with Fusobacterium nucleatum on the malignant transformation of colorectal adenomas. J Biomed Sci. 2022;29(1):88.
44. Bui FQ, Almeida-da-Silva CLC, Huynh B, Trinh A, Liu J, Woodward J, et al. Association between periodontal pathogens and systemic disease. Biomed J. 2019;42(1):27-35.
45. Sparks Stein P, Steffen MJ, Smith C, Jicha G, Ebersole JL, Abner E, et al. Serum antibodies to periodontal pathogens are a risk factor for Alzheimer's disease. Alzheimers Dement. 2012;8(3):196-203.
46. Li F, Ma C, Lei S, Pan Y, Lin L, Pan C, et al. Gingipains may be one of the key virulence factors of Porphyromonas gingivalis to impair cognition and enhance blood-brain barrier permeability: An animal study. J Clin Periodontol. 2024;51(7):818-39.
47. Adams B, Nunes JM, Page MJ, Roberts T, Carr J, Nell TA, et al. Parkinson's Disease: A Systemic Inflammatory Disease Accompanied by Bacterial Inflammagens. Front Aging Neurosci. 2019;11:210.
48. Romano F, Barbui A, Aimetti M. Periodontal pathogens in periodontal pockets and in carotid atheromatous plaques. Minerva Stomatol. 2007;56(4):169-79.
49. Figuero E, Sánchez-Beltrán M, Cuesta-Frechoso S, Tejerina JM, del Castro JA, Gutiérrez JM, et al. Detection of periodontal bacteria in atheromatous plaque by nested polymerase chain reaction. J Periodontol. 2011;82(10):1469-77.

Fig. 1

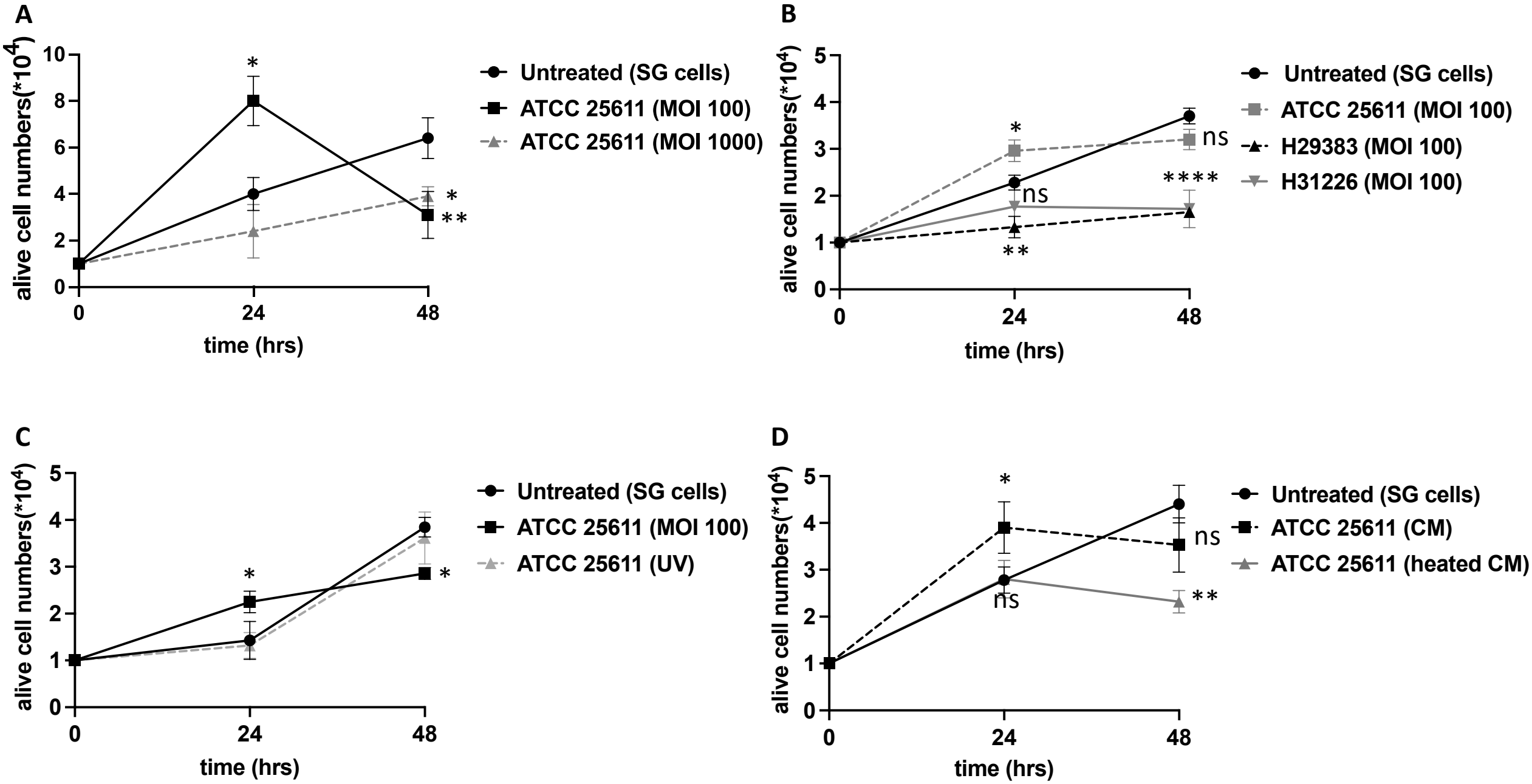
A
alive cell numbers(*10^4)
time (hrs)
Untreated (SG cells)
ATCC 25611 (MOI 100)
ATCC 25611 (MOI 1000)
B
alive cell numbers(*10^4)
time (hrs)
Untreated (SG cells)
ATCC 25611 (MOI 100)
H29383 (MOI 100)
H31226 (MOI 100)
ns
****
C
alive cell numbers(*10^4)
time (hrs)
Untreated (SG cells)
ATCC 25611 (MOI 100)
ATCC 25611 (UV)
D
alive cell numbers(*10^4)
time (hrs)
Untreated (SG cells)
ATCC 25611 (CM)
ATCC 25611 (heated CM)
ns

Fig. 1

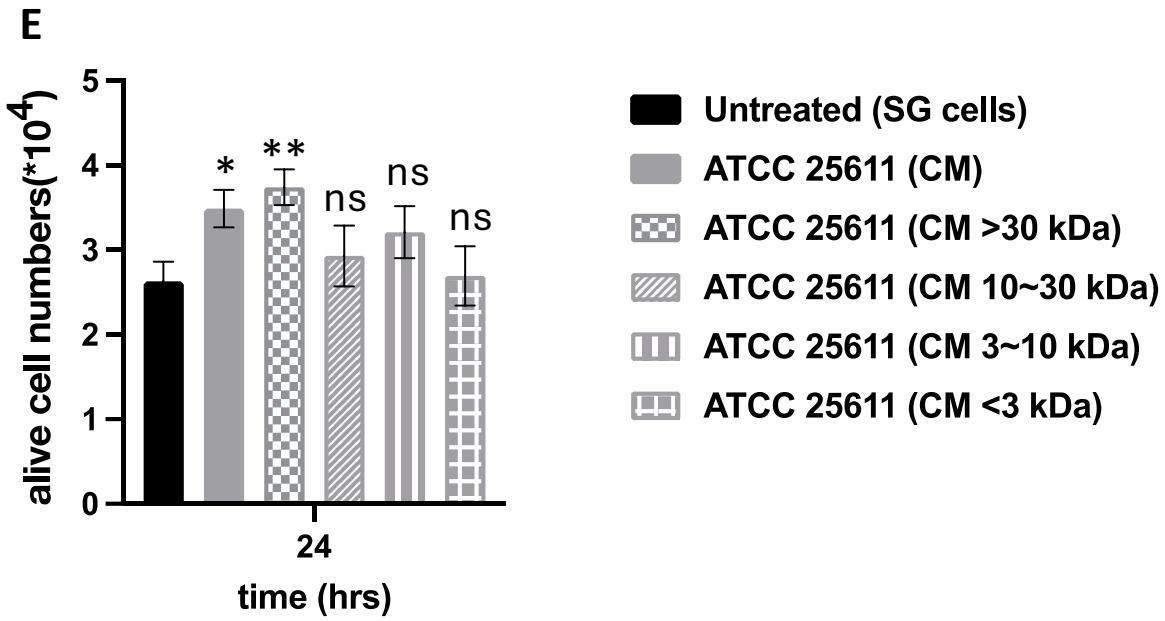
E
alive cell numbers(*10^4)
5
4
3
2
1
0
*
**
ns
ns
ns
24
time (hrs)
Untreated (SG cells)
ATCC 25611 (CM)
ATCC 25611 (CM >30 kDa)
ATCC 25611 (CM 10~30 kDa)
ATCC 25611 (CM 3~10 kDa)
ATCC 25611 (CM <3 kDa)

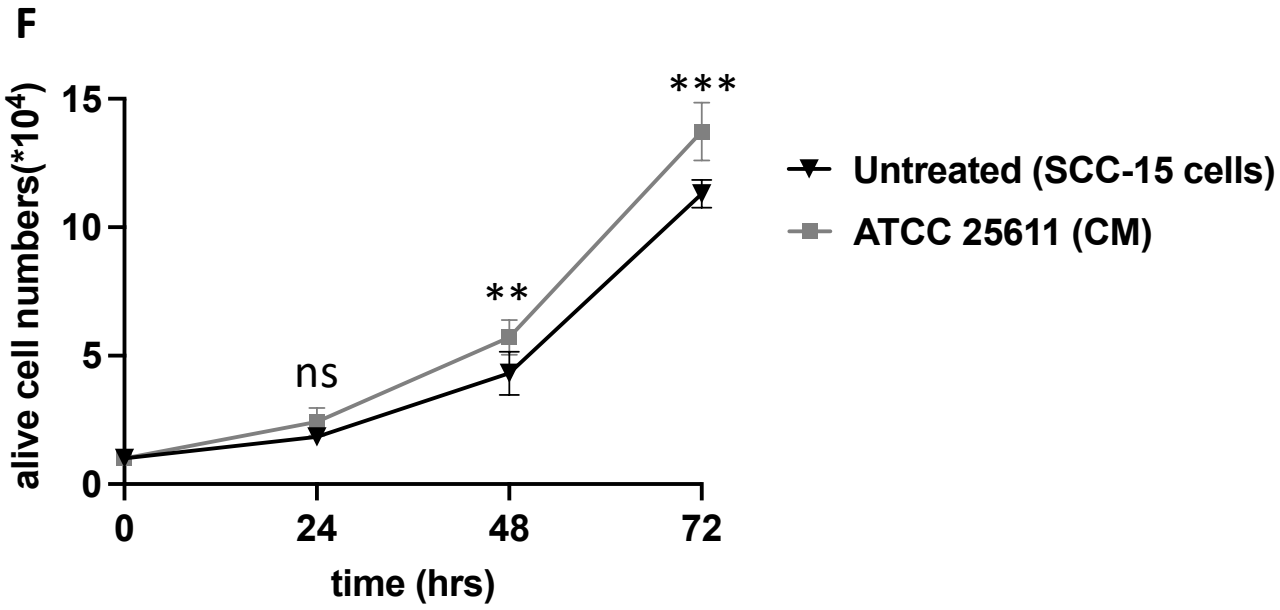
F
alive cell numbers(*10^4)
15
10
5
0
ns
**
***
0
24
48
72
time (hrs)
Untreated (SCC-15 cells)
ATCC 25611 (CM)

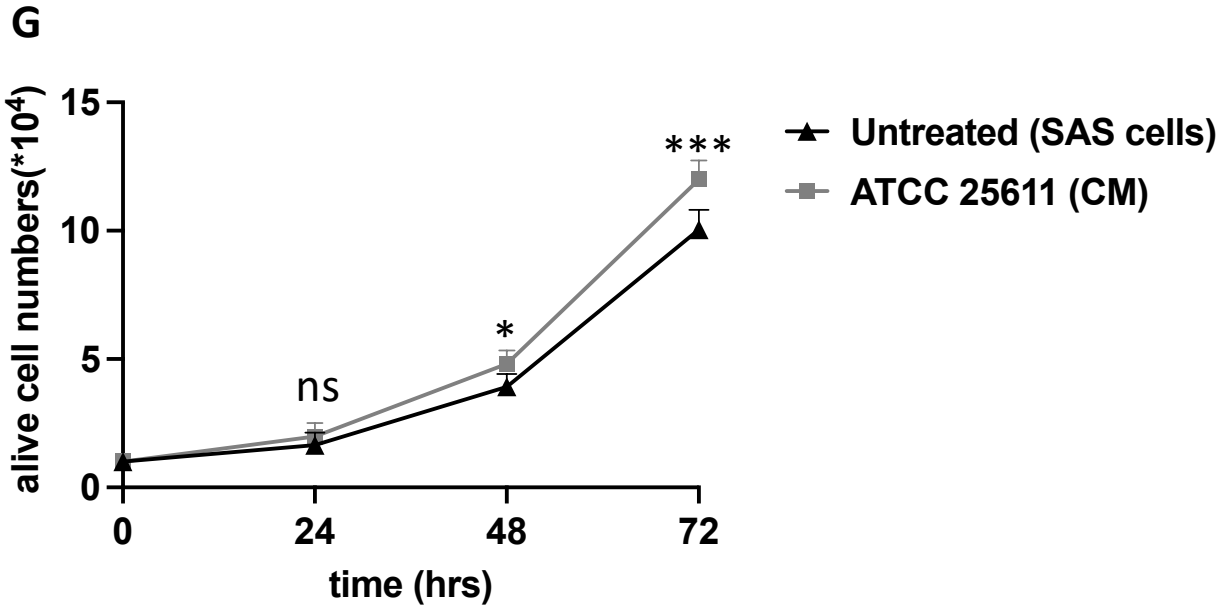
G
alive cell numbers(*10^4)
15
10
5
0
ns
*
***
0
24
48
72
time (hrs)
Untreated (SAS cells)
ATCC 25611 (CM)

Fig. 2

A

Strain	Protein	Prot_acc	Prot_hit_num
ATCC 25611	Interpain A	A0A0D9NCF8 A9J7N5	273 273
H31226		A0A0D9NCF8 A9J7N5 A0A0S3UMK9	21 21 21

13-fold

B

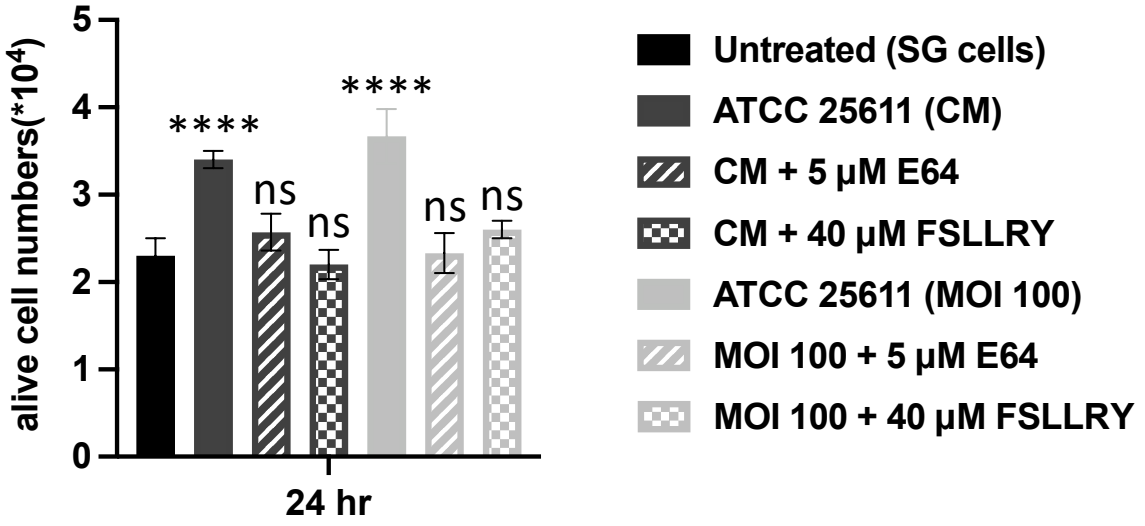

Fig. 2

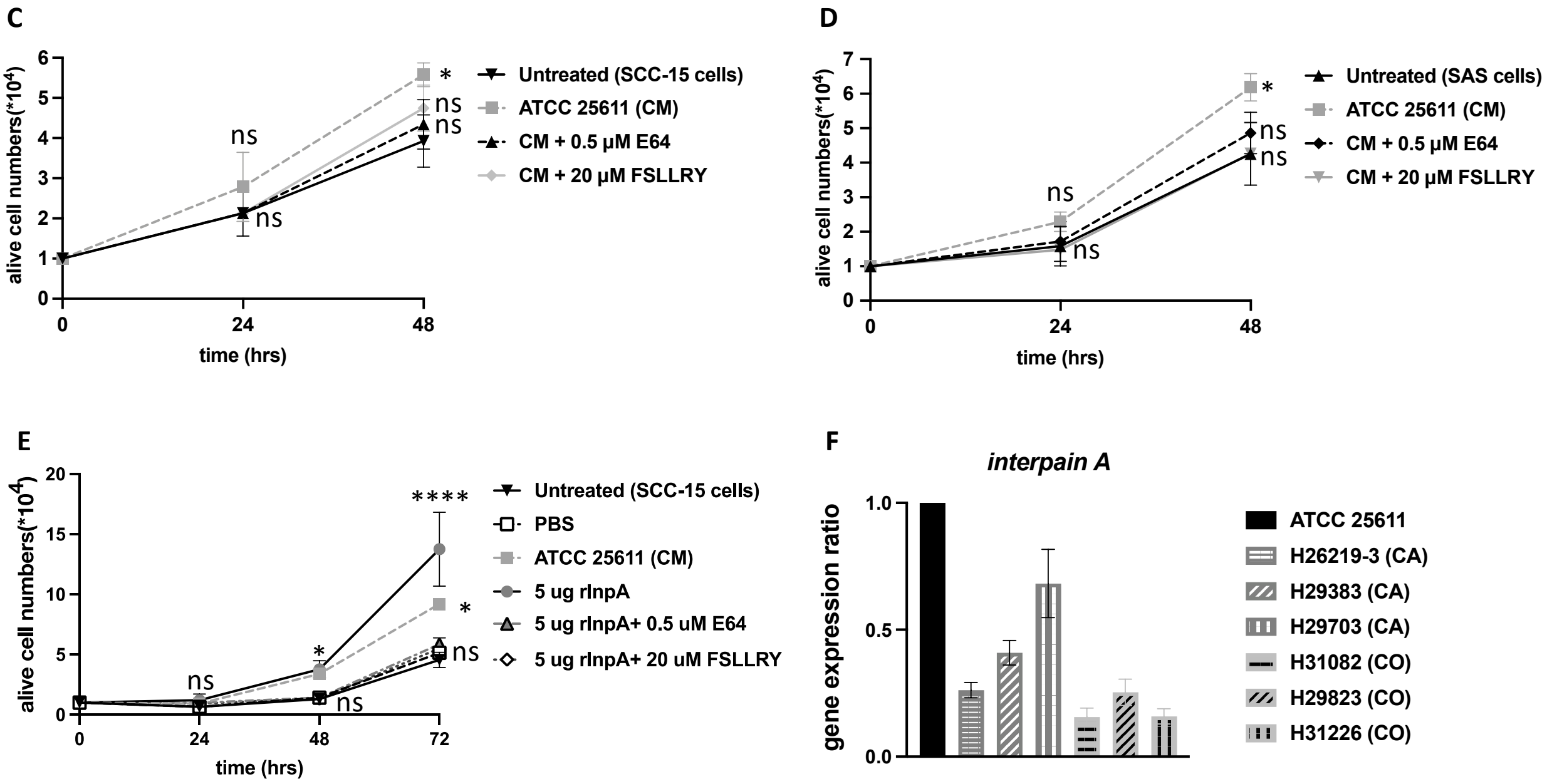
C
alive cell numbers(*10^4)
time (hrs)
Untreated (SCC-15 cells)
ATCC 25611 (CM)
CM + 0.5 μM E64
CM + 20 μM FSLLRY
ns
*
D
alive cell numbers(*10^4)
time (hrs)
Untreated (SAS cells)
ATCC 25611 (CM)
CM + 0.5 μM E64
CM + 20 μM FSLLRY
E
alive cell numbers(*10^4)
time (hrs)
Untreated (SCC-15 cells)
PBS
ATCC 25611 (CM)
5 ug rInpA
5 ug rInpA+ 0.5 uM E64
5 ug rInpA+ 20 uM FSLLRY
****
F
interpain A
gene expression ratio
ATCC 25611
H26219-3 (CA)
H29383 (CA)
H29703 (CA)
H31082 (CO)
H29823 (CO)
H31226 (CO)

Fig. 3

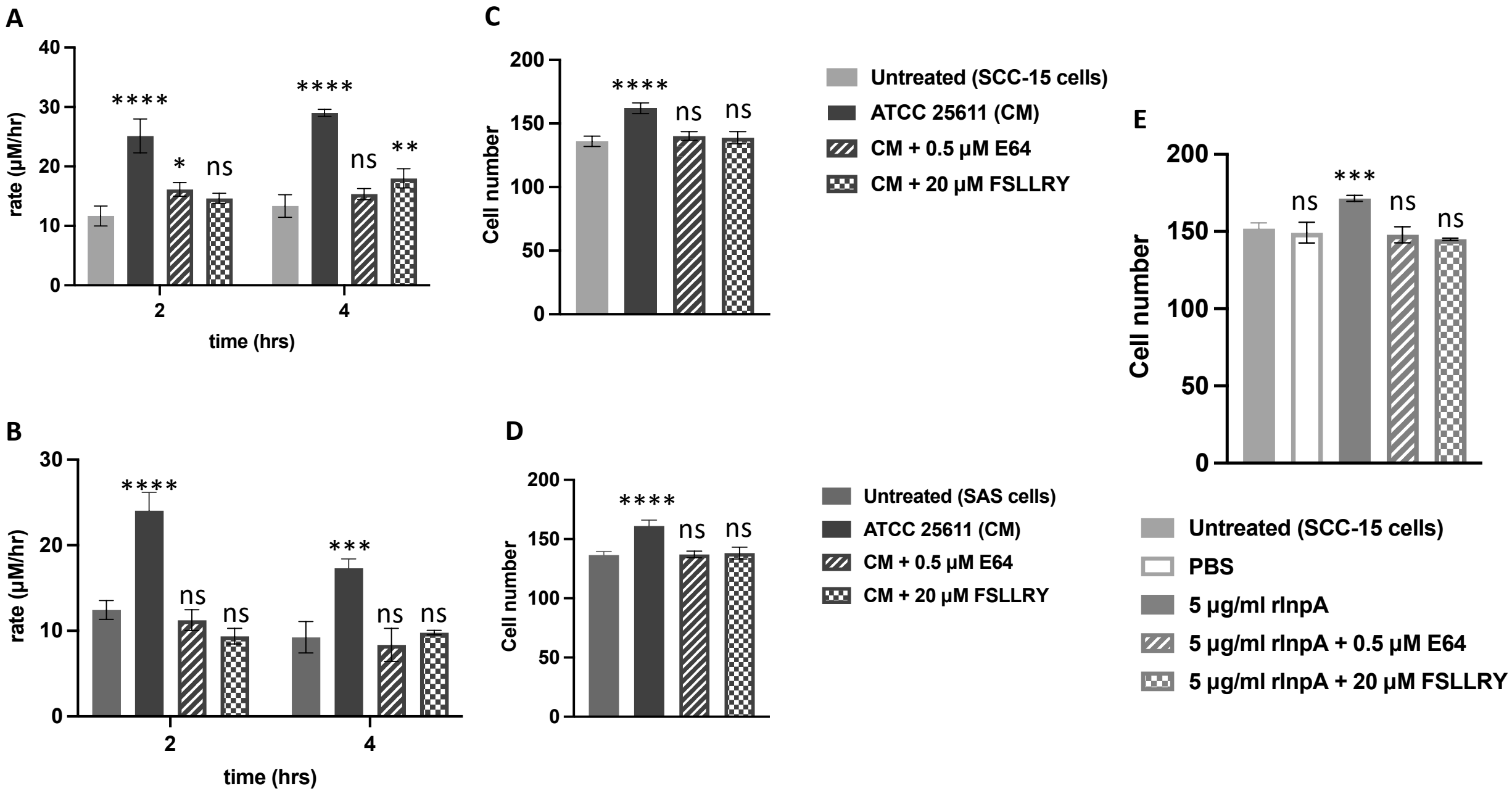
A
rate (μM/hr)
time (hrs)
****
*
ns
****
ns
**
B
rate (μM/hr)
time (hrs)
****
ns
ns
***
ns
ns
C
Cell number
****
ns
ns
D
Cell number
****
ns
ns
Untreated (SCC-15 cells)
ATCC 25611 (CM)
CM + 0.5 μM E64
CM + 20 μM FSLLRY
Untreated (SAS cells)
ATCC 25611 (CM)
CM + 0.5 μM E64
CM + 20 μM FSLLRY
E
Cell number
ns
***
ns
ns
Untreated (SCC-15 cells)
PBS
5 μg/ml rInpA
5 μg/ml rInpA + 0.5 μM E64
5 μg/ml rInpA + 20 μM FSLLRY

Fig. 4

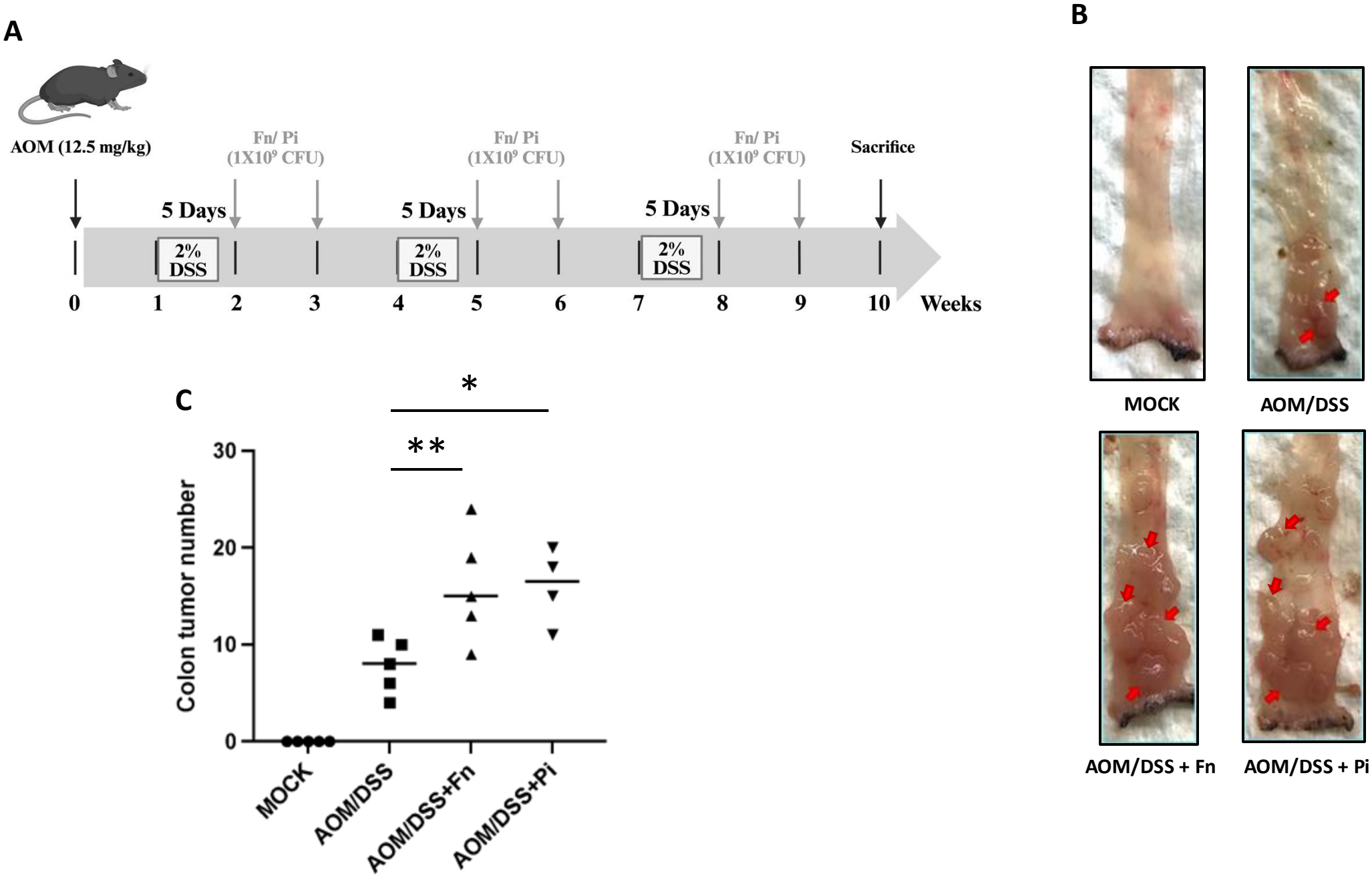
A
AOM (12.5 mg/kg)
Fn/ Pi
(1X10⁹ CFU)
Fn/ Pi
(1X10⁹ CFU)
Fn/ Pi
(1X10⁹ CFU)
Sacrifice
5 Days
5 Days
5 Days
2% DSS
2% DSS
2% DSS
0 1 2 3 4 5 6 7 8 9 10 Weeks
B
MOCK
AOM/DSS
AOM/DSS + Fn
AOM/DSS + Pi
C
*
**
Colon tumor number
30
20
10
0
MOCK
AOM/DSS
AOM/DSS+Fn
AOM/DSS+Pi